ADVANCES IN TRANSPORTATION STUDIES
An International Journal

Guest Editor: N. Stamatiadis and R. Souleyrette

2024 Special Issue, Vol. 4

Contents

aracne

Advances in Transportation Studies an international Journal 2024 Special Issue, Vol. 4

ISBN 979-12-218-1671-6 – ISSN 1824-5463 – DOI 10.53136/97912218167161 – pag. 3-16

A pilot application of the sliding window screening method on Virginia roadways

H.W. Cho C.-L. Lan

Virginia Transportation Research Council,
530 Edgemont Rd, Charlottesville, VA 22903, USA
email: Hyun.Cho@VDOT.Virginia.Gov

Abstract

This study evaluates the practicality and efficacy of implementing the Highway Safety Manual recommended sliding window method for systemically identifying high-risk segments in the Virginia roadway network. The research proposes a homogeneous segmentation network that maintains consistency in segment characteristics, based on annual average daily traffic and safety performance function types. The sliding window method, executed in Python, was applied to the newly generated homogeneous segments. The evaluation of this method's performance encompassed multiple aspects, including assessment of potential for safety improvement (PSI) values, segment rankings, and ranking of segments with roadway attributes. Further, the study investigated the sensitivity of window size selection to the inherent stochastic nature of crash occurrences. Specifically, smaller window sizes were more effective in identifying localized crash "hotspots," and larger window sizes delivered a more general overview of the entire segment. The study also advises against the use of a single year's ranking for determining high-risk PSI segments, owing to this stochastic variation. The study found that the sliding window method does not exhibit inherent bias toward two roadway attributes: segment length and median presence. The finding mitigates the existing segment length variation problem that is present in the current approach.

Keywords – network screening, sliding window, new segmentation

1. Introduction

Since the implementation of the Highway Safety Manual (HSM) [1], the metric of "excess expected average crash frequency or Potential for Safety Improvement (PSI) with Empirical Bayes (EB) adjustment" has gained widespread acceptance as a performance measure for network screening. While it offers the advantage of addressing regression-to-the-mean bias, it is constrained by the need for safety performance functions (SPFs) tailored to local conditions. Recognizing this, the Virginia Department of Transportation (VDOT) has undertaken various initiatives to develop Virginia-specific safety performance functions (VA-SPFs) [3,4]. Leveraging these VA-SPFs, VDOT has been able to analyze crash numbers on segments and assess the difference between observed and expected crash counts effectively.

The Highway Safety Manual (HSM) introduced three screening methods: simple ranking, sliding window, and peak searching. Each method serves specific purposes: roadway segments undergo screening using either sliding window or peak searching methods, while nodes (intersections) are screened using the simple ranking method. For performance measures such as expected average crash frequency that apply SPF on segments, those segments can be treated as nodes by normalizing length of those segments, which unit of performance measure is crashes per mile. Consequently, the simple ranking method becomes applicable to both nodes and segments. The simplicity of the simple ranking method is its notable strength. However, when applied to length-normalized segments, its results may not be as dependable as those generated by other segment screening methods. This is particularly evident in scenarios involving extremely short segments, where the inclusion of such segments could introduce a significant degree of randomness in identifying high-risk sites.

The sliding window screening method conceptually shifts a window of a fixed length along the road segment from start to end, advancing in increments of a specific size. The chosen performance measure for screening the segment is applied to each window position. For all windows relevant to a given segment, the one with the highest potential for crash frequency reduction (i.e., with the highest PSI value) is identified and used to represent the entire segment. After all segments are ranked according to their highest subsegment value, segments with the highest PSI value are subjected to detailed investigation to identify potential countermeasures.

Since the implementation of sliding window method was introduced [5], several state DOTs including those in California [6], Connecticut [2], Florida [7], and Texas [8] have studied or implemented the sliding window method for network screening of highway's safety improvement. The purpose of this study was (1) to develop a new homogeneous segmentation network using multiple roadway types in the Virginia roadway network; (2) to develop the HSM-recommended sliding window screening method on the new segmentation network; and (3) to assess the strengths and limitations of the sliding window screening method.

2. Methodology

2.1. Data

Roadway inventory, crash data, Annual Average Daily Traffic (AADT) data, and Safety performance functions (SPFs) were compiled. Five years' worth of crash and AADT data (from 2016 to 2020) was collected. SPFs provide an estimate of average crash frequency for a site based on models that used data from a population of similar sites. SPFs types are categorized by four factors following the Federal Highway Administration's (FHWA) predefined facility subtypes; area type (urban/rural), facility (highway/interstate freeway), median division (divided/undivided), and number of lanes. SPFs are mathematical equations that predicts the number of crashes for a specific site type from variables of AADT and segment length. The general form of a freeway segment SPF is shown as:

$$\mathrm{N} = \mathrm{L} \times \exp^{\alpha} \times \mathrm{AADT}^{\beta 1} \quad (1)$$

where: N= predicted number of crashes at a site per year,

L= segment length (in miles),

α and $\beta 1$ are regression parameters estimated during the modelling process.

Each equation includes an adjustment coefficient to compensate the overrepresentation of crash frequency on shorter segments. The dispersion functional form shown in the following equation:

$$\mathrm{Dispersion} = \mathrm{L}^{\beta_3} \times e^{\gamma} \quad (2)$$

A new segmentation method was developed from the data prepared in this section. This new segmentation method created homogeneous segments in terms of AADT and SPF types, meaning each homogeneous segment shares the same characteristics in terms of AADT, rural/urban, functional class, facility type, divided/undivided, access control, and number of lanes.

2.2. Implementation of sliding window screening method

The application of the HSM recommended sliding window screening method was carried out on the homogeneous segments that were generated in the previous section. Utilizing Python as a computing tool, the HSM-suggested parameters – 0.3 miles for window length (W) and a moving increment of 0.1 miles – were incorporated into each segment to compute the expected crash frequency for each window.

The calculation of excess predicted average crash frequency was performed as follows:

Step 1. Determine the size of the subsegment network and the length of sliding window (W)

The length of sliding window (W) is equivalent to the length of segment (L) for subsequent calculations if it is less than or equal to the overall link length.

Step 2. Calculate the predicted number of crashes by applying appropriate SPFs to each segment.

$$n_{pred.} = L \times \exp^{\alpha} \times AADT^{\beta} \quad (3)$$

where $L =$ segment length (in miles),
$AADT =$ annual average daily traffic,
α and β are regression parameters estimated during the modeling process.

where $n_{pred.}$ is the annual number of all crashes for a segment, AADT is the annual average daily traffic (number of vehicles per day), and L is segment length (mile), which is equivalent to window size.

Step 3. Using the model predictions computed in step 1, compute the calibration factor C_i

$$C_i = \frac{\sum n_{Obs.\_Allsites}}{\sum n_{Pred.\_Allsites}} \quad (4)$$

C_i is calculated by dividing the total number of observed crashes by the total number of predicted crashes, for each year, within the study area.

Step 4. Compute the weights (w). Weight (w) is calculated using dispersion parameter k and the sum of predicted crashes $n_{pred.}$ at the segment.

$$w = \frac{1}{1+(k \times \sum n_{Pred.})} \quad (5)$$

$$k = L^{\beta_3} \times e^{\gamma} \quad (6)$$

where L is segment length (in miles) and β_3 and γ are model parameters for dispersion.

Step 5. Calculate Empirical-Bayes Adjusted expected number of crashes for each segment.

The expected (EB adjusted) number of crashes ($n_{Exp.}$) are determined using the predicted number of crashes ($n_{Pred.}$) from step 1 and the observed number of crashes ($n_{Obs.}$) multiplying the EB weight (w) that is calculated using the sum of predicted crashes at the segment.

$$n_{Exp.} = w \times (n_{Pred.}) \times C_i + (1 - w) \times n_{Obs.} \quad (7)$$

Step 6. Calculate the potential for safety improvement for each segment each year.

Potential for safety improvement (PSI) is an important criterion that measures excess accident frequency, the difference between the expected (EB adjusted) number of crashes ($n_{Exp.}$) and the predicted number of crashes ($n_{Pred.}$).

$$PSI = n_{Exp.} - n_{Pred.} \quad (8)$$

The key variables, specific to each window, obtained through this calculation were stored in a separate file for further examination and analysis.

2.3. Assessment of sliding window screening method

The assessment of the sliding window method encompassed several dimensions, which are discussed below:

1. Potential for Safety Improvement Values: The computed PSI values served as a benchmark for identifying high-risk segments that may necessitate safety enhancements (positive PSI values indicate excess accident frequencies). The distribution of PSI values across all network segments provided a holistic image of the reliability of the computed values as well as SPFs. Note that a positive PSI value denotes an excess accident frequency.

2. Ranking of segments. Roadway segments were ranked in both an all-inclusive manner and as categorized by specific roadway types (i.e., interstates, US routes, state routes, and secondary routes). The objective was not only to pinpoint the most hazardous segments universally but also to examine the influence of roadway types on segment rankings. An effort was also made to observe the temporal shifts in the risk associated with each roadway segment.

3. Segments Ranks with Other Attributes: The ranks of segments were analyzed in conjunction with attributes such as AADT value associated with each segment. This allowed for a deeper exploration of the relationship between these ranks and specific roadway attributes.

4. Sensitivity Analysis on Model: Window size selection plays a pivotal role in data analysis. The adoption of a smaller window size may prove to be suitable for the identification of localized crash hotspots, and a larger window size can yield a smoothed interpretation of the data. The selection of window size is a crucial consideration as it should be aligned with the spatial scale at which one seeks to analyse and interpret the data. Consequently, the necessity for conducting experiments with various window sizes and assessing their impacts on the final analytical results become apparent.

3. Analysis and results

3.1. Data

This section summarizes and compares the RNS road network and the new segmentation network in terms of the characteristics of segment length and matched crashes. Table 1 shows the detailed characteristics of the RNS road network and crash data for the Fredericksburg District of VDOT. The table includes the total number of segments, total and average length of segments, minimum and maximum length of segments, and total crashes by route type. It should be noted that for the limited access freeways, only the mainlines are included; ramps are excluded. The Fredericksburg District of VDOT has only one corridor (I-95) of interstate highway. For secondary roads, only routes from VDOT's Top 100 PSI list were selected. It was found that the minimum length of segments on the RNS road network was about 0.001 miles and the maximum length of segments was 3.36 miles. The average length of segments was about 0.2 miles.

Table 2 shows characteristics of the new segmentation network of the Fredericksburg district. For comparison to the RNS data, the table also includes the total number of segments, total and average length of segments, minimum and maximum length of segments by route type. It was found that the minimum length of the new segmentation network was about 0.01 miles, which is due to split by rural/urban designation. For Interstate highways, the minimum length was 0.5 miles, which is the length of a weaving section. The maximum length of segments varied from 6.02 to 9.84 miles by type, and the average length of segments was about 1.5 miles. One may note that discrepancies exist in the total segment length between Tables 1 and 2 due to the removal of certain data entries from the RNS database. These discrepancies are attributable to the existence of segments with non-primary directions (applicable to both State Routes and Secondary Roads) in the original RNS data, which have been excluded in the new segmentation.

Tab. 1 - Summary of the RNS road inventory used of Fredericksburg District of VDOT

Roadway Type	Total Number of Segments	Total Length (Miles)	Average Length of Segments (Miles)	Minimum Length of Segments (Miles)	Maximum Length of Segments (Miles)	Total Crashes (2016-2020)
Interstates (IS)	300	93.7	0.31	0.001	3.36	7,161
US Routes (US)	1,457	272.8	0.19	0.001	2.40	3,489
State Primary Routes (SR)	2,297	478.5	0.21	0.001	2.59	3,723
Secondary Roads (SC)	985	190.9	0.19	0.001	2.12	1,620
Total	5,039	1035.9	0.21	0.001	3.36	15,993

RNS = Roadway Network System.

Tab. 2 - Summary of new segment network of Fredericksburg District

Roadway Type	Total Number of Segments	Total Length (Miles)	Average Length of Segments (Miles)	Minimum Length of Segments (Miles)	Maximum Length of Segments (Miles)
Interstates	71	93.7	1.32	0.5	7.10
US Routes	169	272.8	1.61	0.01	9.84
State Primary Routes	250	476.6	1.91	0.01	9.74
Secondary Roads	184	191.1	1.04	0.01	6.02
Total	674	1034.2	1.53	0.01	9.84

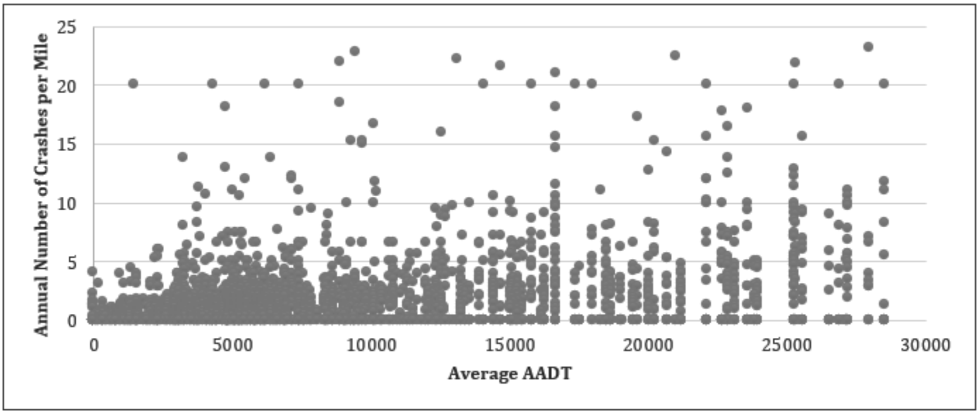

(a) RNS network

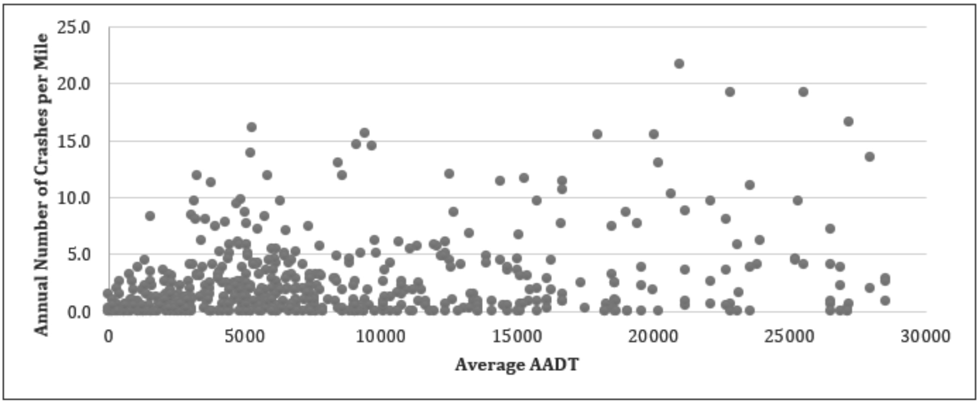

(b) New Segmentation Network

Fig. 1 - Scatterplot of annual number of crashes per mile and average AADT: (a) RNS network; (b) new segmentation network. AADT = Annual Average Daily Traffic; RNS = Roadway Network System

Figure 2 shows the annual number of crashes by mile point on I-95 NB for the RNS network and the new segmentation network. For the 48.9-mile corridor, there are 181 segments for the RNS network, whereas there are only 35 segments for the new segmentation network. It should be noted that columns are mapped by start mile point of segment, and segments with zero crashes are not shown in the plot. On the RNS network, 55 of 181 segments have no crashes; on the new segmentation network, no segments have zero crashes.

The new segmentation network, which combines the densely fragmented RNS network segments that have the same roadway and traffic characteristics, overcomes certain drawbacks of the RNS network such as the presence of very short (0.001 miles) segments, large number of segments with no crashes, and biased relationships between crashes per mile and AADT. However, as Figure 2(b) shows, the new segmentation network may have very long segment lengths, so it may be difficult to detect precise crash and PSI hotspot locations. Creating subsegments of the new segmentation network using a designated size such as 0.1 miles solves that problem. Figure 3 shows the annual number of crashes distributed by mile point in the same corridor using 0.1-mile subsegments of the new segmentation network.

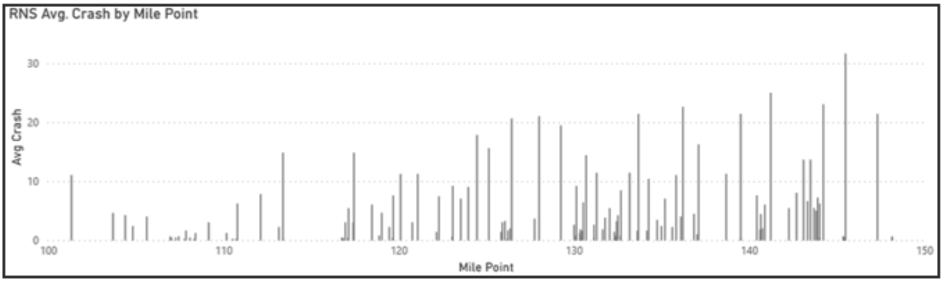

(a) RNS Network

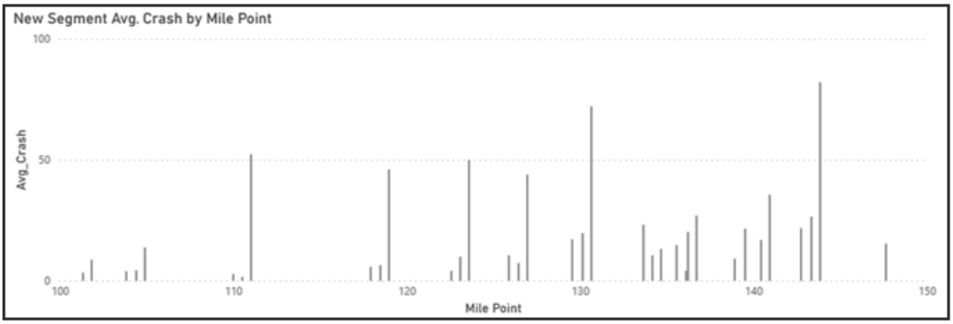

(b) New Segmentation Network

Fig. 2 - Distribution of annual number of crashes by mile point for I-95 NB: (a) RNS network; (b) new segmentation network. RNS = Roadway Network System

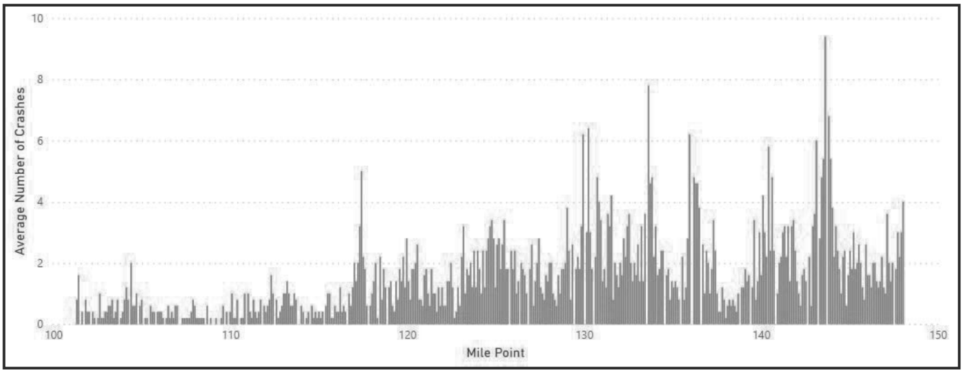

Fig. 3 - Distribution of annual number of crashes by mile point for I-95 NB using 0.1-mile subsegments of the new segmentation network

Figure 1 shows scatterplots of the annual number of crashes per mile and five-year average AADT, which is traditionally used for the representation of an SPF. It should be noted that for visual clarity the figure does not show all data points; points with an AADT between 30,000 and 85,000 and more than 25 crashes per mile per year are hidden. In Figure 1(a), the RNS network plot shows vertical lines since the average AADT could be the same on different segments in a corridor. The new segmentation network, shown in Figure 1(b), eliminates those. It can also be noted from the figure that the new data points from the new segmentation is also less noisy.

3.2. Implementation of sliding window screening method

3.2.1. Potential for safety improvement values

Potential for safety improvement (PSI) values, as derived from the sliding window method, serve as the most critical safety performance measurement; notably, a positive PSI value implies an excess crash frequency. Figure 4 illustrates the distribution of both the empirical Bayes adjusted crash frequency (represented by blue columns) and predicted crash frequency (signified by red columns) for the northbound I-95 corridor subdivided into 0.1-mile subsegments for the year 2018. Within each homogeneous segment, the predicted number of crashes remains consistent, correlating with their constant AADT values. The differences in the predicted number of crashes and the Empirical Bayes adjusted number of crashes (denoted as the disparity in height between the blue and red columns) constitutes the PSI value at that particular point.

3.2.2. Ranking of segments

This section describes a comparison of segment ranks obtained using the HSM-recommended sliding window screening method across various years, in conjunction with some derived measures. These measures were based on the frequency of a segment's appearance in the top riskiest segments. Table 3 shows the top 20 segments based on the frequency of a segment's appearance in the top 10 riskiest segments.

Each row in Table 3 corresponds to a segment (Link ID) identified by a route name and its start and end mile points (Start MP and End MP). Along with ranks for each year (columns labeled PSI 2016 Rank through PSI 2020 Rank), the table presents three additional derived measures: the number of times a segment is in the top 5 riskiest segments, the number of times a segment is in the top 10 riskiest segments, and the sum of the ranks for the segment from 2016 to 2020. Notably, the top 5 and top 10 segments account for the top 0.7% and top 1.5%, respectively, of the riskiest segments among all roadways in the study area (totalling 674 segments). Table 3 reveals certain segments consistently ranking at the top, such as US_15, whereas others, such as IS_32, showcase a considerable variation in ranking from year to year. Some segments, such as IS_21, exhibit a clear trend over time, rising from rank 661 in 2016 to the top position in 2020.

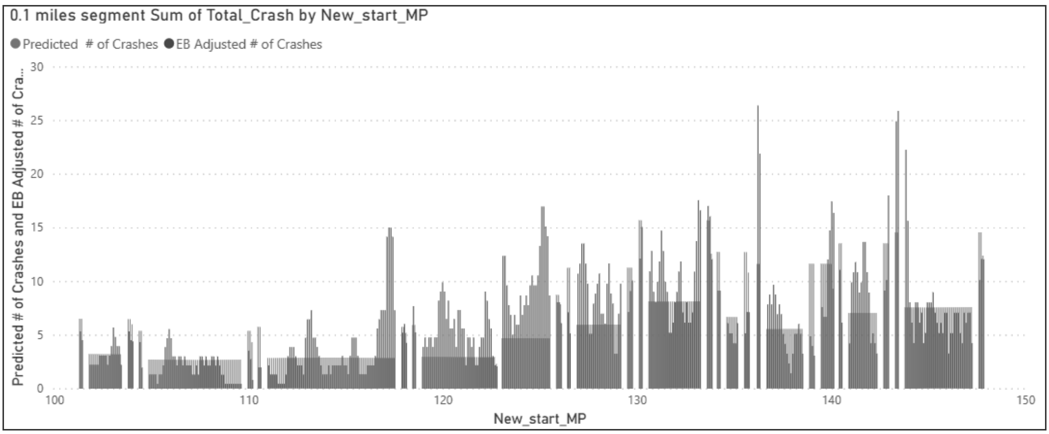

Fig. 4 - Year 2018 Empirical Bayes adjusted and predicted number of crashes distribution by mile point for I-95 NB of 0.1 miles Subsegment Network (window size = 0.3).

Tab. 3 - Yearly breakdown of ranking for top 20 PSI segments and associated derived measures

Link ID	Route Name	Start MP	End MP	PSI 2016 Rank	PSI 2017 Rank	PSI 2018 Rank	PSI 2019 Rank	PSI 2020 Rank	# of Year in Top 5	# of Year in Top 10	Sum of Rank
US_15	US-1	142.29	143	1	1	5	2	2	4	5	11
IS_71	IS-95 NB	141.13	143.63	8	6	3	5	4	2	5	26
IS_74	IS-95 SB	144.66	147.66	5	8	6	6	25	0	4	50
IS_33	IS-95 NB	143.34	143.84	2	5	9	105	35	1	3	156
IS_59	IS-95 SB	133.2	134.1	20	43	7	1	5	1	3	76
IS_72	IS-95 SB	143.63	144.16	204	10	1	3	3	3	3	221
SR_11	SR-3	30.48	31.57	4	4	14	17	6	2	3	45
SR_12	SR-3	31.57	31.91	3	7	2	24	12	2	3	48
IS_34	IS-95 NB	143.84	147.64	15	21	8	4	18	1	2	66
IS_75	IS-95 SB	147.66	148.22	17	2	4	18	654	2	2	695
US_21	US-1	143.96	144.93	7	9	45	51	33	0	2	145
IS_14	IS-95 NB	123.09	125.89	9	15	13	15	24	0	1	76
IS_20	IS-95 NB	130.65	133.65	29	30	12	9	10	0	1	90
IS_21	IS-95 NB	133.65	134.166	661	665	30	16	1	1	1	1373
IS_32	IS-95 NB	142.74	143.34	14	3	23	116	658	1	1	814
IS_60	IS-95 SB	134.1	134.66	21	625	179	244	7	0	1	1076
IS_8	IS-95 NB	111.02	117.92	28	49	18	40	8	0	1	143
SC_104	SC-711	0	1.14	18	17	15	7	16	0	1	73
SC_131	SC-610	9.4	10.49	6	11	24	10	11	0	1	62
SC_133	SC-610	10.63	10.84	80	18	21	8	26	0	1	153

MP = Mile Point; PSI = potential for safety improvement.

The data suggest significant yearly variation in segment ranking. Hence, relying solely on a single year's rank to identify the top PSI segments is not advisable. Further, a segment that has a year with minimal crashes and thus a lower rank (i.e., a large rank number) could result in the segment having a large sum of rank over the years, leading to its potential exclusion (for example, segment IS_21 has a sum of rank of 1373 whereas it topped the list in 2020). In contrast, screening segments based on the frequency of a segment's appearance in the top 5 or top 10 riskiest segments appears to be a more viable approach. Any link that appears in the top 5 or top 10 warrants further investigation. The number of segments ever ranked in the top 5 and top 10 are 11 and 21, respectively, which is a manageable size for closer scrutiny.

3.2.3. Segments ranks with other attributes

This following section undertakes an analysis of the interrelation between segment rankings and particular roadway attributes including AADT, segment length, roadway divisions (divided/undivided), and urban/rural designation. A certain relationship between the segment rank and AADT value was identified. Figure 5 provides a visual depiction of the yearly breakdown of the Top 5 and Top 10 PSI segments along with their corresponding AADT Ranks on US Routes (Figure 5(a)) and State Routes (Figure 5(b)) from year 2016 to 2020. The segments featuring in the top 5 PSI values are marked in magenta, while those within ranks 6 to 10 are colored in dark blue.

An examination of these figures reveals a consistent trend across both US Routes and State Routes, where higher-ranking segments generally associated with higher AADT values. When extending the scope of analysis to include all roadway types, the correlation coefficient between segment rank and AADT value range from -0.06 to -0.13 over the years 2016 to 2020, indicating a weak to mild correlation. However, when the correlation analysis was focused on the top 100 PSI segments, a significantly stronger correlation was observed. Specifically, the correlation coefficients between segment rank and AADT values within this subset ranged from -0.50 to -0.66, thereby suggesting a robust inverse relationship. This correlation evaluation re-affirms that higher-ranking segments tend to associate with higher AADT values.

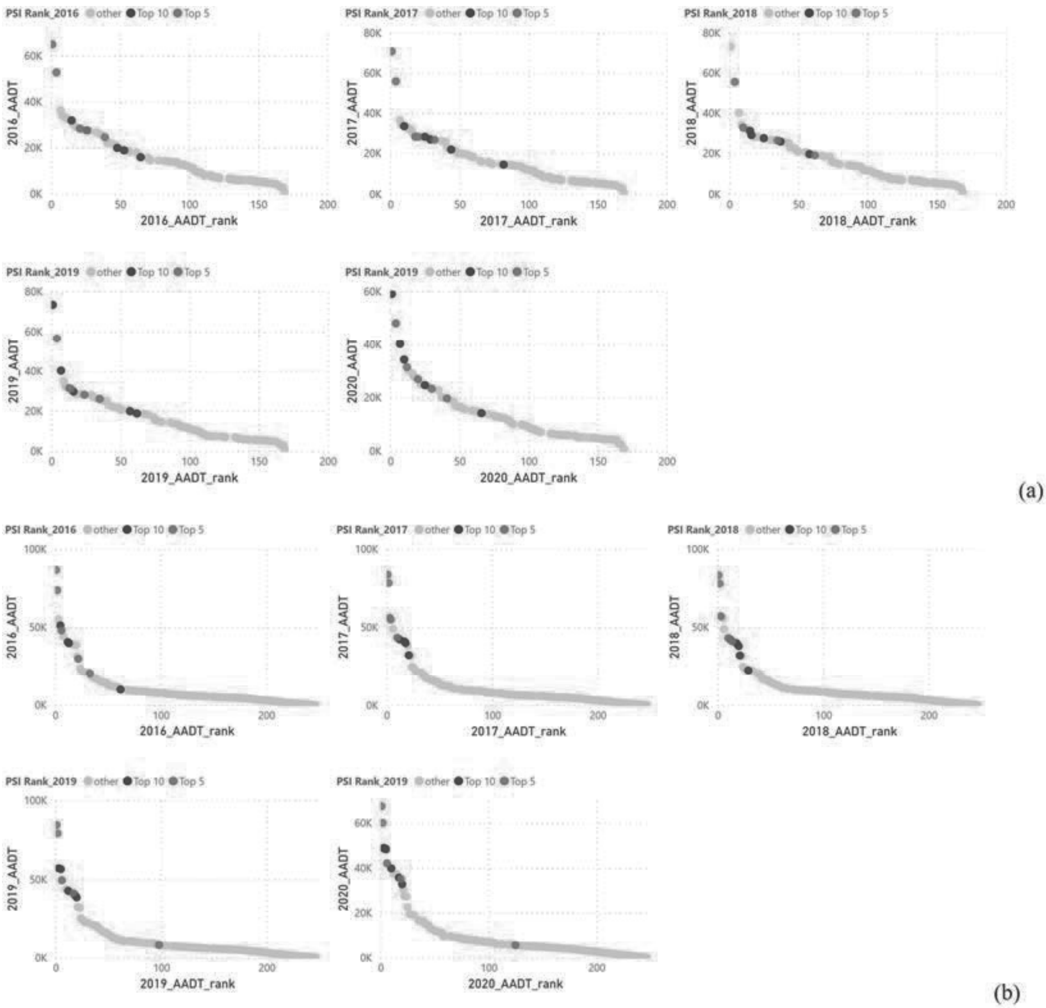

Fig. 5 - The Top 5 and Top 10 PSI segments with their corresponding AADT ranks for the years 2016 to 2020 on (a) US Routes and (b) State Routes

There are several potential explanations for this observation. First, higher AADT values are often linked with major arterials, which may have more access points or other influencing factors not directly captured by SPFs without crash modification factors (CMFs). It is important to note that the calculation of PSI values in this study solely considers the application of SPFs without using CMFs. This approach is chosen to maintain consistency with current practices. Second, the SPFs for these roadway types may not be well-calibrated and might either require re-calibration or the establishment of new SPF types.

In addition, no significant correlations were observed between roadway divisions and segment ranks, as indicated by correlation values from -0.08 to -0.03 throughout the years 2016 to 2020. Upon analysis, it was determined that no specific correlations exist between segment ranks and variables such as segment length and roadway division. This observation is positive, as it implies that the HSM-recommended sliding window method does not exhibit inherent biased towards these variables. For example, the method doesn't show any bias towards shorter segments, which is often a concern in existing real-world practices.

3.2.4. Sensitivity analysis on model

This section performed a sensitivity analysis that encompassed a variety of window sizes, ranging from 0.3 to 0.7 miles with 0.1-mile increments. The intent was to assess how PSI values and segment ranks changed across these different window sizes. Table 4 shows a comparison of segments from all roadway types, ranking highest in the year 2016 across various window sizes. Each row represents a segment (Link ID), identified by a route name and the start and end mile points (Start MP and End MP), along with its 2016 rank for different window sizes, ranging from 0.3 to 0.7 miles (columns W=3 through W=7). It is worth noting that in cases where the length of a segment falls short of the predetermined window size set for the sliding window screening method, the window size for that particular segment is set to match its length. In other words, the entire segment is treated as a single window for analysis purposes. By comparing Tables 3 and 4, it becomes evident that the variation in segment ranks among different window sizes is smaller than that across different years. For instance, the segment US_15 consistently holds the #1 rank across all window sizes from W=3 to W=7, showing zero variation. The maximum rank differences for any segment across window sizes is 54 positions, as seen with IS_70, which shifts from rank 19 at window size W=3 to rank 73 at W=5 and W=7. Most of the top segments maintained a relatively stable rank regardless of window size within a specific year. In contrast, the maximum rank differences across years reach up to 664 positions (see Table 3). For example, IS_21 changed from rank 665 in 2017 to rank 1 in 2020.

Apart from the maximum rank difference, the result also shows that variations in ranks due to different window sizes are minimal compared to the fluctuations observed across different years. By calculating the variances of rankings for all 20 segments across five window sizes within the same year, we found an average variance of approximately 1.76. In contrast, the average variance of rankings across five years was substantially higher at around 266.3. This result confirms that the variance in rankings across years is significantly greater than the variance across window sizes. The above observations show that temporal factors have a much greater impact on PSI segment rankings than window size.

Tab. 4 - Top 20 PSI segments ranking across various window sizes

Link ID	Route Name	Start MP	End MP	PSI 2016 Rank W=3	PSI 2016 Rank W=4	PSI 2016 Rank W=5	PSI 2016 Rank W=6	PSI 2016 Rank W=7
US_15	US-1	142.29	143	1	1	1	1	1
IS_33	IS-95 NB	143.34	143.84	2	4	6	6	6
SR_12	SR-3	31.57	31.91	3	3	4	4	4
SR_11	SR-3	30.48	31.57	4	2	2	2	2
IS_74	IS-95 SB	144.66	147.66	5	5	3	3	3
SC_131	SC-610	9.4	10.49	6	7	9	8	9
US_21	US-1	143.96	144.93	7	6	5	5	5
IS_71	IS-95 SB	141.13	143.63	8	9	12	11	7
IS_14	IS-95 NB	123.09	125.89	9	12	7	7	8
US_52	US-1	159.81	161.27	10	11	10	10	10
IS_24	IS-95 NB	135.566	136.11	11	18	22	36	37
US_99	US-17	182.35	184.66	12	10	8	9	11
IS_73	IS-95 SB	144.16	144.66	13	20	35	32	34
IS_32	IS-95 NB	142.74	143.34	14	13	21	60	62
IS_34	IS-95 NB	143.84	147.64	15	14	11	13	17
US_97	US-17	171.61	172.66	16	17	20	18	19
IS_75	IS-95 SB	147.66	148.22	17	8	13	24	25
SC_104	SC-711	0	1.14	18	15	14	15	15
IS_70	IS-95 SB	140.63	141.13	19	31	73	71	73
IS_59	IS-95 SB	133.2	134.1	20	23	34	20	20

PSI = potential for safety improvement; MP = mile point.

4. Discussion

The sliding window method presents several key advantages, which are as follows:

1. Standardization across variable segment lengths: The sliding window method provides a standardized way to analyse roadway segments of different lengths. This standardization mitigates inherent bias based on segment length.
2. Adaptability to crash distributions: One of the strengths of the sliding window method lies in its ability to account for diverse spatial crash distributions. By adjusting the window sizes, traffic engineers can refine their focus to identify either localized hotspots or broader trends across an entire segment.
3. Mitigation of randomness: The sliding window method can smooth out the randomness inherent in crash occurrences, making it a more reliable tool for safety analysis. For example, a specific 0.1-mile unit may rank high in some years due to the stochastic nature of crashes, making the effectiveness of the simple ranking method contingent on this randomness. By reducing the impact of such random fluctuations, the sliding window method delivers a more consistent and reliable analysis.

4. Flexibility for various safety measures: The sliding window method can align with different safety improvement measures. Some measures are designed to improve safety across a longer segment, while others are intended as spot treatments for specific locations. Traffic engineers can adjust the window size to help identify the most appropriate segments for different types of improvement measures.

Overall, these strengths highlight the sliding window method's capacity to provide a more flexible and reliable analysis of roadway safety.

5. Conclusions

- The new homogeneous segmentation network developed in this study overcame several limitations of the current roadway network, such as biased representation of crash rate per mile due to the presence of very short segments (<0.01 mile). However, more effort was required to create the new segmentation network.
- When the HSM-recommended sliding window screening method is employed, a smaller window size can be more effective in detecting localized crash hotspots. Conversely, a larger window size facilitates a smoother and more comprehensive overview of the segment.
- The HSM-recommended sliding window method did not demonstrate inherent bias toward roadway attributes including segment length, or median presence. However, segments with higher rankings (PSI values) were generally found to be associated with higher AADT values.
- The stochastic nature of crash occurrences can cause considerable fluctuations in segment rankings over different years. Consequently, the use of a single year's ranking to identify the top PSI segments is not recommended due to this inherent variability.

References

1. American Association of State Highway and Transportation Officials (2010) Highway Safety Manual. Washington, DC.
2. Connecticut Transportation Safety Research Center (2020), Connecticut Roadway Safety Management System User Manual.
3. Garber, N.J., and Rivera, G. (2010) Safety Performance Functions for Intersections on Highways Maintained by the Virginia Department of Transportation. VTRC 11-CR1. Virginia Transportation Research Council, Charlottesville.
4. Garber, N.J., Philip, R.H., and Conrad, G. (2010), Development of Safety Performance Functions for Two-Lane Roads Maintained by the Virginia Department of Transportation. VTRC 10- R25. Virginia Transportation Research Council, Charlottesville.
5. Harwood, D.W., Torbic, D.J., Richard, K.R., and Meyer, M.M. (2010), SafetyAnalyst: Software Tools for Safety Management of Specific Highway Sites. FHWA-HRT-10-063. Federal Highway Administration, Washington, DC.
6. Kwon, O.H., Park, M.J., Yeo, H., and Chung, K. (2013), Evaluating the Performance of Network Screening Methods for Detecting High Collision Concentration Locations on Highways. Accident Analysis and Prevention, Vol. 51, pp. 141-149.
7. Matata, F., Salum, J. H., and Alluri, P. (2023), Exploring the Choice of Sliding Window Parameters for Identifying Hazardous Roadway Segments. In Proceedings of the 102nd Annual Meeting of the Transportation Research Board, Washington, DC.

8. Tsapakis, I., Holik, W., Geedipally, S., Samant, S., and Dixon, K. (2019), Statewide Implementation of Innovative Safety Analysis Tools in Identifying Highway Safety Improvement Projects. Report 5-6912-01-R1. Texas A&M Transportation Institute, College Station.

Advances in Transportation Studies an international Journal 2024 Special Issue, Vol. 4

ISBN 979-12-218-1671-6 – ISSN 1824-5463 – DOI 10.53136/97912218167162 – pag. 17-30

Exploring freeway crash duration by the latent class accelerated hazard model with heteroskedasticity effect

F. Chiang* Y.R. Zhe C.Y. Hsu

Department of Transportation and Communication Management Science, National Cheng Kung University, University, No. 1, University Rd. Tainan City 701, Taiwan,
**corresponding author; email: chongson0425@gs.ncku.edu.tw*

Abstract

Managing traffic crashes on freeways presents a substantial challenge due to their unpredictable and nonrecurrent nature, often resulting in prolonged delays in traffic. To investigate the factors influencing freeway traffic crash duration in Taiwan, this study analyzed data encompassing 47,497 instances of freeway crashes between 2018 and 2021 to mitigate these detrimental effects. Additionally, this study introduced a novel approach, the generalized log-gamma-based latent class-accelerated hazard model with heteroskedasticity effects (HLCAH), to explore these factors. The HLCAH model categorizes crashes into three types based on crash variables: “medium duration with a long initial period,” “long duration with a short initial period,” and “short duration with a medium initial period.” Furthermore, to account for heteroskedasticity effects, the model parameterizes the probability distribution (location, scale, and shape parameters) with exogenous crash covariates. This approach not only contributes to a deeper understanding of freeway traffic crash duration but also has significant implications for enhancing freeway rescue efficiency. The model findings underscore the importance of incorporating latent classes and parameterizing distribution parameters. This research concludes with actionable insights aimed at reducing crash duration.

Keywords – freeway crash duration, latent class survival analysis, Generalized Log-Gamma, heteroscedasticity

1. Introduction

Road crashes, characterized by their unpredictable and sporadic occurrence, disrupt normal traffic flow, leading to prolonged lane occupation and reduced road service levels. This results in traffic congestion, significant travel delays, and increased greenhouse gas emissions. High-traffic highways, such as freeway, particularly those frequented by heavy commercial vehicles such as trucks, tankers, and container trucks, face heightened risks of secondary collisions. Informing road users about expected clearance times can mitigate these impacts by allowing them to adjust travel plans preemptively, choosing alternative routes, or delaying or cancelling trips. An accurate estimation of crash duration is crucial for providing reliable information to support these decisions.

A substantial body of research has focused on mitigating the impact of severe crashes through effective strategies, typically modelling crash clearance duration [1, 2]. Initially, ordinary regression methods based on statistical theory were popular due to their simplicity [3-6]. However, the skewed nature of actual crash clearance duration data often does not conform to normal distribution assumptions [5, 6]. Therefore, the adoption of distributions such as log-normal or log-logistic distributions has been preferred for describing crash duration [1, 7-9]. Many studies have employed survival models to explore road crash duration, categorized into parametric, semiparametric, and nonparametric models depending on their treatment of time dependence [10-14].

Survival models derived from probability theory typically include density, survival, and hazard functions, which vary across different probability distributions to suit the nature of the data [8, 9, 15]. Recent advancements have integrated heterogeneity terms into models such as accelerated failure time (AFT) regression, which enhances model fit and statistical power while maintaining robust results [15, 16]. AFT models, which are extensively utilized in crash duration research, incorporate variables such as weather conditions, vehicle characteristics, crash types, road surroundings, and location types to provide reliable estimates [1, 7, 17-22].

Despite these advancements, the application of latent class-accelerated failure time models in traffic crash duration studies remains limited [23, 24]. Such models can capture heterogeneity across crash duration patterns by grouping data into segments and estimating parameters for each segment. The selection of AFT models is often guided by distributional assumptions [25]. For instance, Lee and Timmermans [26] proposed a generalized log-gamma (GLG) distribution-based latent class AFT model (LCAH) for analyzing daily trip activity duration, which offers flexibility compared to standard distributions such as exponential, Weibull, and log-normal distributions [27].

An ongoing concern is the investigation of heteroscedasticity effects in distribution parameters, such as scale and shape, in crash clearance studies, an area less explored except in select literature [28]. To address these issues comprehensively, this study introduces the latent class survival model with heteroscedasticity effects (HLCAH) within the context of freeway crash clearance times in Taiwan. An empirical case study focuses on the Taiwanese freeway network, which has experienced a notable increase in vehicle kilometers and crashes in recent years[1], emphasizing the need for continuous enhancement of crash-clearance practices. This research aims to classify freeway crash duration patterns and identify key features to inform effective improvement strategies.

2. The proposed model

In our case study, the specific time (t) for a crash is the time when the staff in the National Freeway Regional Traffic Control Center (TCC) identify a crash, record its occurrence (the time of origin), and report the crash clearance (the endpoint) after the recovery of all roadway lanes. In some cases, TCC staff may report that a crash has been cleared without further investigation when informed of the crash, as the vehicles involved have left the scene or are on the road shoulder and, therefore, have no impact on traffic flow. This is because more than 90% of freeway crashes are property damage only (PDO) crashes. Furthermore, our definition has the advantage of not eliminating any data due to censored or truncated issues.

Let y be random variables denoting the natural logarithm of the crash duration, $Ln(T)$. The HLCAH model for the natural logarithm of crash duration time y with relevant covariates X can be derived because we assume that K distinct homogeneous patterns (latent classes) exist in the

[1] The total vehicle kilometers on Taiwanese freeways will have increased to 32,400 million by 2021, an increase of 10% compared to 2012 (29,468 million vehicle kilometers). The number of crashes will increase from 17,586 in 2012 to 32,865 in 2021, an increase of 84.6%. Of these crashes, 92.4% are PDO (property damage only). There were 97 traffic accidents per day on average during the year 2021.

heterogeneous population of the sample. Given that a specific crash duration belongs to class k ($k = 1..., K$), the natural logarithm of the crash duration y can be formulated as follows:

$$y = \beta_k X_k + \tilde{\sigma}\varepsilon_k \tag{1}$$

where X_k represents the vector of risk covariates for class k, with the corresponding estimated coefficient vector β_k and a parameterized function $\tilde{\sigma}$ depicting the scale parameter. ε_k is a vector of random variables with a standard baseline distribution for class k. $\tilde{\sigma}$ is a fixed parameterized function that is used to depict the scale across ε_k. Notably, there is a distinction between the LCAH and the HLCAH. The current formulation specifies the scale parameter as a linear function ($\tilde{\sigma} = e^{\tau\eta}$) with covariates η and corresponding parameters τ.

Subsequently, the probability density function (p.d.f.) of the random variable $\varepsilon_k(X_k; \beta_k) = \frac{1}{\tilde{\sigma}}\{Y - \beta_k X_k\}$ is expressed as:

$$f(y) = \frac{1}{\tilde{\sigma}} f'\{\varepsilon_k(X_k; \beta_k)\} \tag{2}$$

where $f'(\varepsilon_k)$ is a standard probability distribution function (p.d.f.); the survival function of this distribution takes the form:

$$S(y) = S'\{\varepsilon_k(X_k; \beta_k)\} \tag{3}$$

Moreover, $S'(\varepsilon_k)$ is a fully specified survivor function. Additionally, ε_k is a vector of random variables specific to class k assumed to be the GLG distribution relevant to another parameterized function $\tilde{\lambda} = e^{\gamma\xi}$ depicting the shape parameter across classes as follows:

$$f'(y; \tilde{\lambda}) \begin{cases} \frac{|\tilde{\lambda}\,|}{\tilde{\sigma}\Gamma(\tilde{\lambda}^{-2})} (\tilde{\lambda}^{-2})^{(\tilde{\lambda}^{-2})} exp\left[\tilde{\lambda}^{-2}\left(\tilde{\lambda}\,\varepsilon_k - exp(\tilde{\lambda}\,\varepsilon_k)\right)\right], \tilde{\lambda} \neq 0 \\ \frac{1}{\sqrt{2\pi\tilde{\sigma}^2}} exp\left[-\frac{1}{2}{\varepsilon_k}^2\right], \qquad \tilde{\lambda} = 0 \end{cases} \tag{4}$$

In addition to the log-logistic distribution, the HLCAH can degenerate to represent various patterns of crash duration, such as the exponential ($\tilde{\lambda}$ =1|$\tilde{\sigma}$ = 1), Weibull ($\tilde{\lambda}$=1), standard gamma ($\tilde{\sigma}$=1), and log-normal ($\tilde{\sigma} \rightarrow 0$) distributions. Moreover, the two parameterizing functions $\tilde{\lambda}$ and $\tilde{\sigma}$ with their covariate vectors η and ξ can also be included to characterize the heteroscedasticity effects of the variance and skewness in the underlying distribution. A noteworthy advantage of the GLG is that we employ it as an accelerated hazard formulation. In addition, the formulation of the survival function is

$$S'(y) = 1 - I\left[\tilde{\lambda}^{-2}, \tilde{\lambda}^{-2}\, exp(\varepsilon_k\tilde{\lambda})\right], -\infty < Z_k < \infty \tag{5}$$

where $I(\lambda, m)$ is specified as an incomplete gamma function:

$$I(\lambda, m) = \frac{1}{\Gamma(\tilde{\lambda}^{-2})} \int_0^m u^{\tilde{\lambda}^{-2}-1}\, e^{-u} du \tag{6}$$

The conditional likelihood function given that the i^{th} crash with relevant covariate vector X_{ik} for a specific class k is:

$$L_{ik} = \frac{1}{\tilde{\sigma}} f'(\varepsilon_{ik}; \tilde{\lambda}) \cdot S'(\varepsilon_{ik}; \tilde{\lambda}) \tag{7}$$

where $\varepsilon_{ik} = \{Ln(T_i) - \beta_k X_{ik}\}/\tilde{\sigma}$; $\tilde{\sigma}_i = e^{\tau\eta_i}$; $\widetilde{\lambda_i} = e^{\gamma\xi_i}$. In the current case, the parametric functions of $\tilde{\sigma}_i$ and $\widetilde{\lambda_i}$ are fixed across classes but vary for each crash. This is because the additional restriction can substantially improve the HLACH estimation efficiency and confirm that more covariates are associated with the two functions. Furthermore, the proposed model assumes the existence of *K* distinct homogeneous latent classes, with any given *i* crash duration belonging to a specific latent class *k* (*k* = 1, 2..., *K*), as expressed:

$$M_{ik} = \frac{exp(\gamma_k Z_i)}{\sum_{k'=1}^{K} exp(\gamma_{k'} Z_i)} \tag{8}$$

where M_{ik} denotes the class probability function that the *i* crash duration belongs to latent class *k* (s=1,2, …, K), which is formulated in a multinomial logit (MNL) type with a linear combination of $\gamma_k \omega$ as well as relevant conditions: $0 \leq M_k \leq 1$, and $\sum M_k$=1. Among them, γ_k is an unknown parameter vector (including a constant) for the segmental variables ω_k exclusive to class k. We arbitrarily set a class for the base, with γ_k=0. Given Eqs. (7) and (8), the complete form of the log-likelihood for all crash durations is given by:

$$\mathbf{Ln}L = \sum_{i=1}^{N} ln\left(\sum_{k=1}^{K} M_{ik} L_{ik}\right)$$
$$= \sum_{i=1}^{N} ln\{\sum_{k=1}^{K} M_{ik} \left[\frac{1}{\tilde{\sigma}} f'(\varepsilon_{ik}; \tilde{\lambda}) \cdot S'(\varepsilon_{ik}; \tilde{\lambda})\right]\} \tag{9}$$

The log-likelihood for the above parameters is used in typical maximum likelihood estimation.

3. The data

Typically, it is unlikely that the freeway TCC staff would be informed of PDO crashes, as there is no need to dispatch a rescue team or provide emergency assistance. However, anyone involved in a crash needs to inform the police, regardless of the severity of the crash. Thus, since most crashes are recorded by the police only (and not by the TCC) the study had to integrate two separate datasets. The TCC, administered by the Taiwan Freeway Bureau, documented the duration of the crash and the information associated with the provision of emergency and rescue services upon the occurrence of the crash. The National Highway Police Bureau (NHPD) records comprehensive details relating to the factors and characteristics of each crash. The study created a new dataset by screening the matching crash cases between the TCC and NHPB datasets to obtain a complete data set. A coding concatenation method was employed to retrieve each crash in the NPHD and TCC datasets. This involved cross-checking the datasets of both NPHD and TCC crash records, respectively, from 2018 to 2021. As a result, 47,497 crashes were matched in the following analysis.

Figure 1 illustrates the crash duration. The unit of the X-axis is minutes, and the unit of the Y-axis is the number of actual crashes. The mean is 20.8 minutes, with a minimum of 0.5 minutes and a maximum of 650 minutes. The discrepancy in the recorded clearance times is considerable, as it depends on how the TCC staff records the beginning and end times of the crash. If TCC staff fail to confirm a crash in the closed-circuit television monitoring system (CCTV) or with the police following the reporting of a crash, there is a possibility that the crash may be deemed cleared and the case closed with minimal delay. It is common for these staff to be informed of a crash that has been cleared due to the delayed reporting from other road users on the scene.